TÜBİTAK

Turkish Journal of Chemistry

http://journals.tubitak.gov.tr/chem/

Research Article

Turk J Chem
(2022) 46: 1642-1650
© TÜBİTAK
doi:10.55730/1300-0527.3467

L-(+)-Tryptophan methyl ester derived polymeric microbeads as an efficient heterogeneous catalyst for green synthesis of 2-amino-4-(nitromethyl)-4*H*-chromene-3-carbonitriles

Ayşe HALIÇ POSLU[1], Bilgen OSMAN[2], Yunus KAYA[1], Ömer KOZ[1], Gamze KOZ[1,*]

[1]Department of Chemistry, Faculty of Engineering and Natural Sciences, Bursa Technical University, Bursa, Turkey
[2]Department of Chemistry, Faculty of Arts and Science, Bursa Uludağ University, Bursa, Turkey

Received: 04.04.2022 • **Accepted/Published Online:** 19.07.2022 • **Final Version:** 05.10.2022

Abstract: The cross-linked microbeads with average diameter of 106–300 μm, [poly(EGDMA-MATrp)], were obtained by copolymerization reaction of N-methacryloyl-L-(+)-tryptophan methyl ester (MATrp) with ethylene glycol dimethacrylate (EGDMA) and successfully applied as a heterogeneous catalyst in conjugate addition reaction of nitromethane to substituted 2-iminochromenes in aqueous media. A variety of 2-amino-4-(nitromethyl)-4*H*-chromene-3-carbonitriles has been synthesized in good yields. Polymeric microbeads were very durable and reused 5 times without a significant loss of activity. DFT calculations and experimental results revealed the significant role of π-π interactions as well as hydrogen bonding in the reaction mechanism.

Key words: Polymeric microbeads, L-(+)-tryptophan methyl ester, nitromethane addition, π-π interaction, DFT calculation

1. Introduction

Functional polymeric microbeads have found many practical applications in chemical separation and purification, wastewater treatment, bioengineering, materials science, drug delivery systems, and cancer therapy [1-6]. The development of polymeric microbeads as heterogeneous organocatalysts has attracted increasing attention due to the advantages such as easy product isolation and catalyst reusability. Polymeric microbeads have been successfully applied to a variety of organic reactions such as Suzuki Miyaura reaction [7], asymmetric Michael, aldol reactions [8], esterification [9], substitution [10] and A^3 coupling reactions, which is a three-component coupling of aldehyde, amine and alkyne for the synthesis of propargylamines [11]. For example, cinchonidinium salts of core-corona polymer microspheres were applied several times in asymmetric alkylations without loss of the enantioselectivity [12]. Shi and coworkers reported the synthesis and characterization of a polymer microsphere catalyst [13]. Ionic liquid immobilized catalyst was applied in the Knoevenagel condensation of ethyl cyanoacetate and benzaldehyde. The benzaldehyde conversion was maintained at 92% after six times reuse. Polymeric microbeads have a great application potential in many other organic reactions as catalysts because of their mechanical strength and high surface area. The additional advantage of polymeric microbeads is the ability to functionalize their surface area with hydrophobic and hydrophilic groups, which play an active role in catalytic transition states.

Osman et al. used N-methacryloyl-L-(+)-tryptophan methyl ester (MATrp) monomer to prepare polymeric microbeads for removal [14, 15] and solid phase extraction [16-18] of some aromatic organic contaminants from aqueous solutions. Poly(ethylene glycol dimethacrylate N-methacryloyl-L-(+)-tryptophan methyl ester) [poly(EGDMA-MATrp)] microbeads were effectively used to remove diethyl phthalate from aqueous solution [19]. The results of these studies showed that the microbeads have a high affinity for aromatic compounds owing to hydrophobic interactions such as π-π stacking between MATrp residues of cross-linked polymer and target analytes. The importance of π-π interactions in transition states (TS) of the catalytic reactions have been emphasized in some recent studies [20-24]. As noncovalent interactions have been the main forces effective on catalytic transition states, we decided to investigate the efficiency of [poly(EGDMA-MATrp)] polymeric microbeads in an organic reaction containing hydrophobic substrates such as chromenes and reveal a mechanistic explanation including π-π interactions.

* Correspondence: gamze.koz@btu.edu.tr

Chromenes are an important class of heterocyclic compounds, widely distributed in natural products. They possess a wide range of biological activities such as anticancer [25], antimicrobial and antifungal [26], antioxidant [27] and anti-HIV [28]. A number of methods using homogeneous [29-31] and heterogeneous catalysts [32-36] have been developed to synthesize functionalized 4*H*-chromenes owing to their importance. We have reported an enantioselective method using a Schiff base-Cu(II) catalyst [37] and a Lewis base catalyzed method for the synthesis of rasemic 2-amino-4-(nitromethyl)-4*H*-chromene-3-carbonitriles from 2-iminochromenes [38]. However, this is the first report on the use of a heterogeneous catalyst in nitromethane additions to 2-iminochromenes. We also present the crucial role of π-π interactions in transition state of the reaction depending on both computational and experimental results.

2. Materials and Methods

All solvents/reagents were obtained commercially from Fluka and Sigma Aldrich and used as purchased. Silica gel F254 (Merck 5554) precoated plates were used for monitoring. A 400 MHz Bruker NMR spectrometer and a Thermo-Nicolet 6700 FT-IR spectrometer was used for NMR and FT-IR analysis, respectively. Polymeric microbeads were analyzed with scanning electron microscopy (Carl Zeiss/Gemini 300). Melting points (mp) were recorded with an electro thermal digital mp apparatus. 2-iminochromenes (**1a**-**m**) were synthesized by a pyrrolidine catalyzed method and known compounds were characterized according to reported mp and 1H NMR data [37-40]. The 6-I substituted 2-iminochromene (**1l**) was not stable at room temperature so it was used as crude in the addition reaction without isolation but the addition product (**2l**) was isolated and fully characterized.

2.1. Synthesis of [Poly(EGDMA-MATrp)] microbeads

The suspension polymerization technique was used to prepare [Poly(EGDMA-MATrp)] microbeads as described in our previous report [14]. EGDMA and MATrp were used as a cross-linker and a monomer, respectively. Polymerization mixture was prepared by dispersing the organic phase including EGDMA (5 mL), MATrp (4 mL), and toluene (10 mL) in aqueous phase prepared via dissolution of 200 mg poly(vinyl alcohol) (PVA) in deionized water (50 mL). After addition of 2,2'-azobisisobutyronitrile (AIBN) (100 mg), the mixture was polymerized at 85 °C with a 600 rpm stirring rate for 8 h. The unreacted residues were washed with excess amount of water and ethanol. The resulted microbeads were dried in a vacuum oven at 50 °C. A Carl Zeiss/Gemini 300 scanning electron microscope was used to monitor the physical morphology of the microbeads.

2.2. Synthesis of 2-iminochromenes (1a-m)

Malononitrile (5 mmol) and the corresponding aromatic aldehyde (5 mmol) were dissolved in a mixture of MeOH:H_2O (3:1) (4 mL) and a catalytic amount of pyrrolidine (0.75 mmol) was added to the mixture. The product precipitated and filtered, washed with 3:1 MeOH:H_2O and dried in a vacuum oven.

*2-Imino-8-nitro-2H-chromene-3-carbonitrile (**1i**, $C_{10}H_5N_3O_3$)*

Yield 56%; mp 204 °C (decomp.); R_f = 0.48 (ethyl acetate/hexane, 1:1); 1H NMR (400 MHz, DMSO-d_6): δ (ppm) 9.37 (bs, 1H, NH), 8.47 (s, 1H, H4), 8.20–8.17 (dd, J_1 = 1.2, J_2 = 8.0 Hz, 1H, ArH), 7.90–7.88 (dd, J_1 = 1.6, J_2 = 8.0 Hz, 1H, ArH), 7.42 (t, J = 8.0 Hz, 1H, ArH). 13C NMR (DMSO-d_6, 100 MHz): δ (ppm) 161.2, 146.7, 146.4, 144.9, 141.6, 134.9, 124.6, 124.4, 120.5, 105.9. FT-IR (neat): $\bar{\nu}$ = 3270, 2238, 1662, 1519, 1231 cm^{-1}. Anal. Calcd. for: $C_{10}H_5N_3O_3$ (%):C, 55.82; H, 2.34; N, 19.53; Found: C, 56.73 ; H, 2.24 ; N, 19.78.

*8-Bromo-2-imino-2H-chromene-3-carbonitrile (**1j**, $C_{10}H_5BrN_2O$)*

Yield 50%; mp 170 °C (decomp.); R_f = 0.53 (ethyl acetate/hexane, 1:2); 1H NMR (400 MHz, DMSO-d_6): δ (ppm) 9.14 (bs, 1H, NH), 8.38 (s, 1H, H4), 7.87–7.85 (dd, J_1 = 1.6, J_2 = 8.0 Hz, 1H, ArH), 7.60–7.58 (dd, J_1 = 1.6, J_2 = 7.6 Hz, 1H, ArH), 7.20 (t, J = 7.6 Hz, 1H, ArH). 13C NMR (DMSO-d_6, 100 MHz): δ (ppm) 150.4, 150.3, 146.5, 137.0, 129.1, 125.4, 119.1, 114.9, 108.3, 105.2. FT-IR (neat): $\bar{\nu}$ = 3292, 3231, 2227, 1663, 1593, 1199 cm^{-1}. Anal. Calcd. for: $C_{10}H_5BrN_2O$ (%):C, 48.22; H, 2.02; Br, 32.08; N, 11.25, Found: C, 49.56; H, 2.06; N, 10.97.

2.3. Synthesis of 2-amino-4-(nitromethyl)-4*H*-chromene-3-carbonitriles (2a-m)

[Poly(EGDMA-MATrp)] microbeads (5mg) and the corresponding 2-iminochromene (**1a-m**) (0.25 mmol) were added to the solution of nitromethane (0.75 mmol) in 5:1 methanol:H_2O (1 mL). The mixture was stirred at room temperature until the corresponding 2-iminochromene was consumed. Methanol was removed by rotary evaporator and the crude product was extracted to ethyl acetate. The organic phase was dried over Na_2SO_4, filtered, and concentrated under reduced pressure to afford the crude product. Column chromatography was used to purify the crude product. The previously reported 4*H*-chromene-3-carbonitriles were characterized using 1H NMR literature data and melting points [37-43].

*2-Amino-8-hydroxy-4-(nitromethyl)-4H-chromene-3-carbonitrile (**2e**, $C_{11}H_9N_3O_4$)*

Yield 51%; mp 173 °C; R_f = 0.43 (ethyl acetate/hexane, 1:1); 1H NMR (400 MHz, DMSO-d_6): δ(ppm) 9.81 (bs, 1H, OH), 7.06 (bs, 2H, NH_2), 6.94 (t, J = 7.6 Hz, 1H, ArH), 6.84–6.81 (dd, J_1 = 1.2, J_2 = 8.0 Hz, 1H, ArH), 6.70–6.68 (dd, J_1 = 0.8, J_2 =

7.6 Hz, 1H, ArH), 4.74–4.70 (dd, J_1 = 5.6, J_2 = 12.4 Hz, 1H, CH_2NO_2), 4.63–4.59 (dd, J_1 = 5.6, J_2 = 12.0 Hz, 1H, CH_2NO_2), 4.24 (t, J = 5.6 Hz, 1H, H4). 13C NMR (100 MHz, DMSO-d_6): δ(ppm) 162.3, 145.2, 138.1, 124.5, 120.6, 119.9, 117.6, 115.5, 80.8, 50.0, 35.0. FT-IR (neat): $\bar{\nu}$ = 3473, 3361, 3206, 2189, 1549 cm^{-1}. Anal. Calcd. for: $C_{11}H_9N_3O_4$ (%):C, 53.44; H, 3.67; N, 17.00; Found: C, 53.61; H, 3.68; N, 15.91.

*2-amino-8-nitro-4-(nitromethyl)-4H-chromene-3-carbonitrile (**2i**, $C_{11}H_8N_4O_5$)*

Yield 31%; mp 152–154 °C; R_f = 0.65 (ethyl acetate/hexane, 1:1); 1H NMR (400 MHz, DMSO-d_6): δ(ppm) 7.94–7.92 (dd, J_1 = 1.6, J_2 = 8.4 Hz, 1H, ArH), 7.71–7.69 (dd, J_1 = 1.2, J_2 = 8.0 Hz, 1H, ArH), 7.41 (bs, 2H, NH_2), 7.38 (d, J = 8.0 Hz, 1H, ArH), 4.92–4.87 (dd, J_1 = 4.8, J_2 = 12.8 Hz, 1H, CH_2NO_2), 4.77–4.72 (dd, J_1 = 4.8, J_2 = 12.8 Hz, 1H, CH_2NO_2), 4.45 (t, J = 4.8 Hz, 1H, H4). 13C NMR (400 MHz, DMSO-d_6): δ(ppm) 161.1, 141.8, 138.2, 133.2, 124.6, 124.4, 122.5, 118.9, 80.3, 50.3, 34.3. FT-IR (neat): $\bar{\nu}$ = 3421, 3327, 2190, 1645, 1519 cm^{-1}. Anal. Calcd. for: $C_{11}H_8N_4O_5$ (%):C, 47.83; H, 2.92; N, 20.28, Found: C, 47.18; H, 2.81; N, 18.55.

*2-Amino-6-iodo-4-(nitromethyl)-4H-chromene-3-carbonitrile (**2l**, $C_{11}H_8IN_3O_3$)*

Yield 38%; mp 196 °C; R_f = 0.35 (ethyl acetate/hexane, 1:2); 1H NMR (400 MHz, $CDCl_3$): δ(ppm) 7.62–7.60 (dd, J_1 = 2.0, J_2 = 8.4 Hz, 1H, ArH), 7.49 (d, J = 2.0 Hz, 1H, ArH), 6.80 (d, J = 8.8 Hz, 1H, ArH), 4.83 (bs, 2H, NH_2), 4.62–4.58 (dd, J_1 = 4.8, J_2 = 12.4 Hz, 1H, CH_2NO_2), 4.55–4.50 (dd, J_1 = 6.4, J_2 = 12.4 Hz, 1H, CH_2NO_2), 4.30–4.27 (dd, J_1 = 4.8, J_2 = 6.4 Hz, 1H, H4). 13C NMR (100 MHz, $CDCl_3$): δ(ppm) 161.8, 149.5, 138.5, 136.6, 121.4, 118.9, 118.7, 88.4, 79.9, 53.2, 34.4. FT-IR (neat): $\bar{\nu}$ = 3442, 3325, 3209, 2918, 2202, 1649, 1531 cm^{-1}. Anal. Calcd. for: $C_{11}H_8IN_3O_3$ (%):C, 37.00; H, 2.26; N, 11.77, Found: C, 37.16; H, 1.98; N, 11.21.

2.4. DFT calculations

Density functional theory (DFT) with the wB97X-D method as applied in the GAUSSIAN 09 program package was conducted for the calculations. Dispersion correction for energy barrier and reaction heat were estimated with the wB97X-D method reported by Grimme [44], as DFT poorly describes dispersion effects. All calculations and harmonic frequencies to find transition states (one imaginary force constant only) or local minima (all positive force constants) of the structures were calculated with the 6-311++G(d,p) basis set in the gas phase.

3. Results and discussion

The [poly(EGDMA-MATrp)] microbeads were synthesized according to the literature (Figure 1) [14].

The cross-linked microbeads were obtained in a spherical form with the size range of 106–300 μm in diameter. SEM images of the microbeads are shown in Figure 2.

The [poly(EGDMA-MATrp)] microbeads were used as the heterogeneous catalyst in the model reaction between nitromethane and **1a** (Table 1).

The best results were obtained in aqueous media (entry 4, 5) and the reaction yields were very poor in polar aprotic solvents (entry 6-8) and toluene. The catalyst loading was examined in water and 90% yield was obtained with 5 mg use of [poly(EGDMA-MATrp)] microbeads (entry 4). Then we investigated the substrate scope of the reaction. As the yields of the first experiments performed with substituted 2-iminochromenes in water were moderate, we carried out the reactions in a mixture of methanol:water (5:1) (Table 2).

A series of 2-amino-4-(nitromethyl)-4*H*-chromene-3-carbonitrile (**2a**-**m**) was synthesized with moderate to good yields (31-95 %) with both, electron-donating and electron-withdrawing substituents on the aromatic ring. In general, reactions of the substrates with electron-donating substituents were high yielding in short reaction times (**2c**, **2d**, **2g**, **2h**) while the electron-withdrawing substrates dramatically decreased the reaction rate (**2i**). These results were attributed to the significant role of π-π interactions in aqueous media between substrates and catalyst as the electron withdrawing substituents weaken π stacking interactions by decreasing the pi electron density of the aromatic ring. Regardless of inductive effects in substituted aromatic rings of 2-iminochromenes, the position of the substituents also affected the reaction yields. In general, higher yields were obtained with 6-substituted (**2b**-**d**, **2f**, **2k**) and 7-substituted (**2h**) 2-iminochromenes while lower yields were obtained with 8-substituted 2-iminochromenes (**2e**, **2g**, **2i**, **2j**).

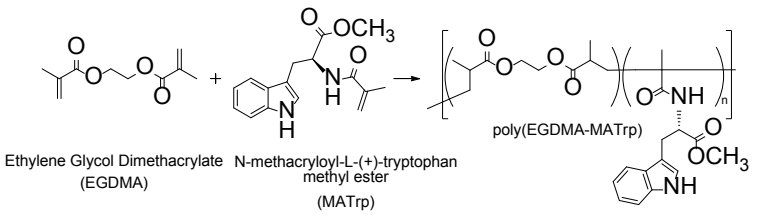

Figure 1. Preparation of poly(EGDMA-MATrp) microbeads.

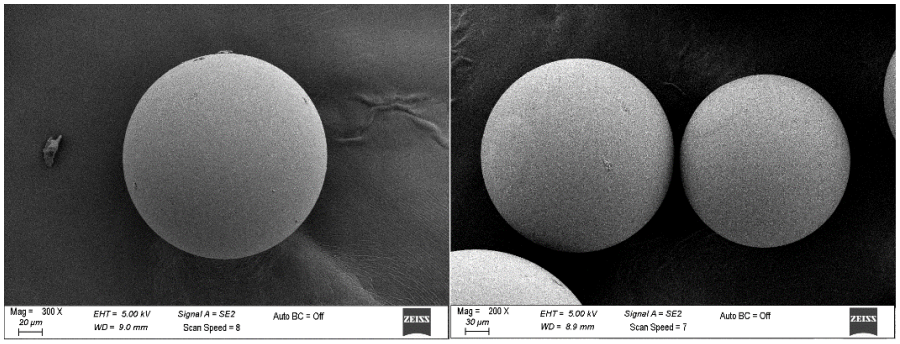

Figure 2. SEM images of [poly(EGDMA-MATrp)] microbeads.

Table 1. [Poly(EGDMA-MATrp)] catalyzed synthesis of 2-amino-4-(nitromethyl)-4*H*-chromene-3-carbonitriles **2a**[a]. Screening of solvents and catalyst loading.

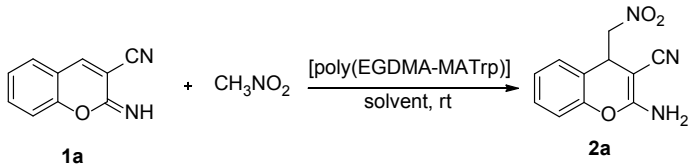

1a **2a**

Entry	Solvent	Time (h)	Yield (%)[b]
1	methanol	18	68
2	ethanol	24	38
3	2-propanol	24	35
4	water	39	90
5	methanol:water (5:1)	24	87
6	chloroform	96	trace
7	acetone	96	trace
8	tetrahydrofuran	96	trace
9	toluene	96	trace
10[c]	water	100	65
11[d]	water	96	30
12[e]	water	120	-

[a]Reaction conditions: 1a (0.25 mmol), nitromethane (0.75 mmol), [poly(EGDMA-MATrp)] (5mg), solvent (1 cm^3). [b]Isolated yields after column chromatography. [c]1 mg catalyst loading. [d]10 mg catalyst loading. [e]without catalyst.

Finally, we tested the reusability of the catalyst in the model reaction between nitromethane and **1a** (Figure 3). The catalyst was centrifuged and separated from reaction medium, washed several times with methanol and air dried after each use.

A distinct decrease was not observed in the activity of the catalyst. The final yield of **2a** decreased only from 87% to 81% at the end of fifth reaction run.

We also performed DFT calculations and suggested a transition state (TS) including all noncovalent interactions. The related potential energy surfaces (PES's) and the optimized structures of the intermediates (IM) and TS along the reaction pathway are shown in Figure 4, while the relative energies of the reactants, IM, TS, and product are given in Table 3.

When the optimized molecular structures are examined, it is observed that the catalyst coordinates to both 2-iminochromene and nitromethane molecules through hydrogen bonding. The formation of intermediate 4-IM via

Table 2. Conjugate addition of nitromethane to 2-iminochromenes[a]. Substrate scope.

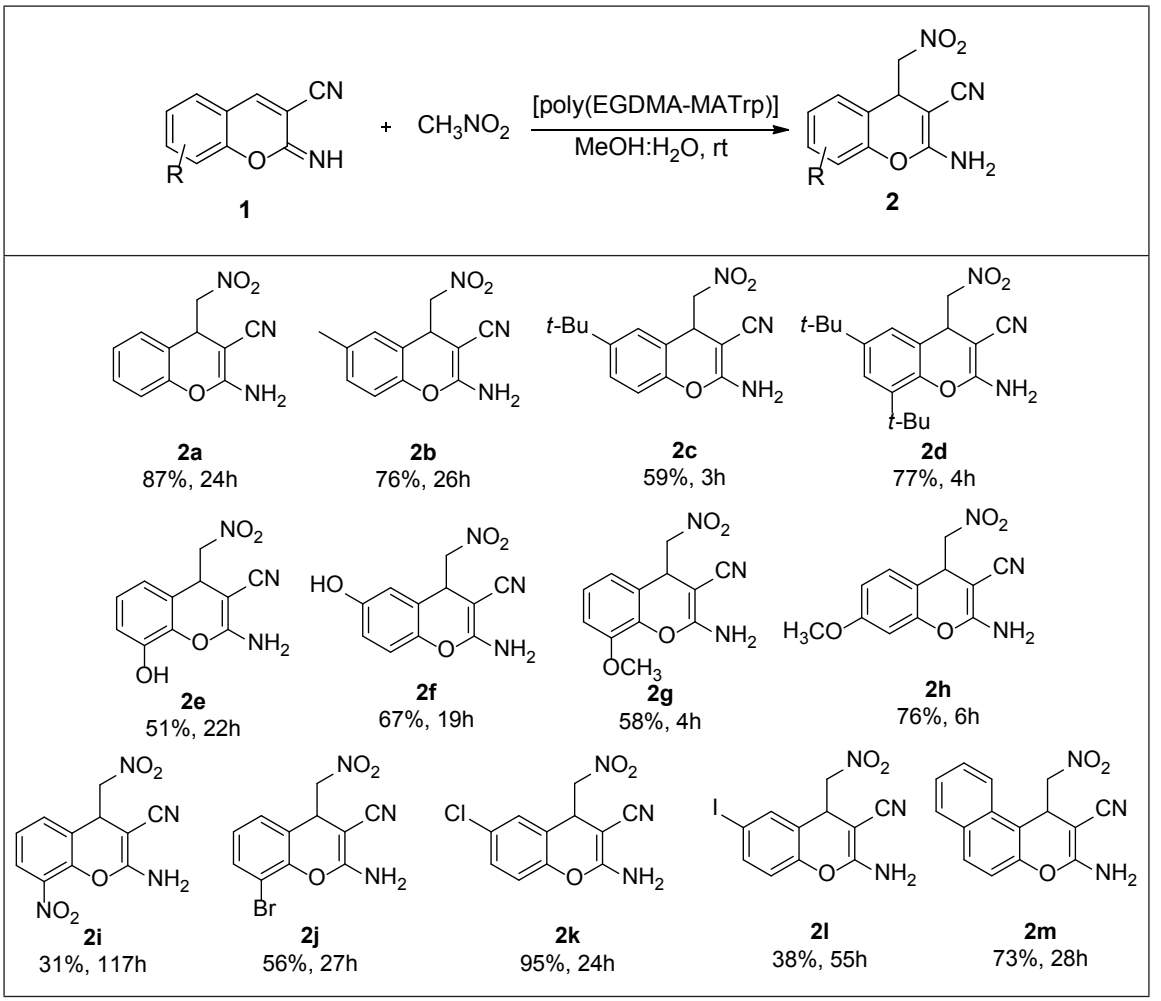

[a]Reaction conditions: **1a** (0.25 mmol), nitromethane (0.75 mmol), [poly(EGDMA-MATrp)] (5mg), MeOH:H_2O (5:1) (1 cm^3). [b]Isolated yields after column chromatography.

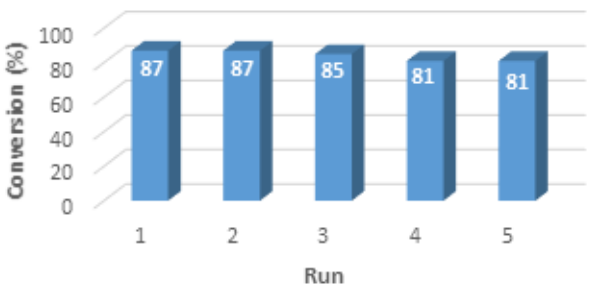

Figure 3. Catalyst reuse; reaction conditions: **1a** (0.25 mmol), nitromethane (0.75 mmol), [poly(EGDMA-MATrp)] microbeads (5 mg), MeOH:H_2O (5:1) (1 mL).

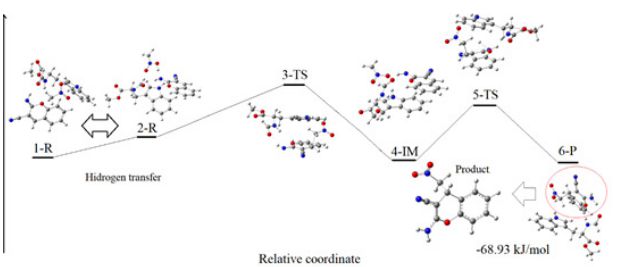

Figure 4. Potential energy diagram & geometry transformations between compound 1-R and compound 6-P, optimized geometries of the reactants, IN, TS, and product calculated by WB97XD/6-311G++(d,p).

Table 3. Negative frequency and relative energy values calculated by WB97XD/6-311G++(d,p) level.

Species	Energy (a.u.)	Relative energy (kJ/mol)	Negative frequency (cm^{-1})
1-R	–1653.29621195	0.00	-
2-R	–1653.28266504	35.56	-
3-TS	–1653.27211882	63.26	–548
4-IM	–1653.28994310	16.45	-
5-TS	–1653.27755360	48.99	–1217
6-P	–1653.32244695	–68.93	-

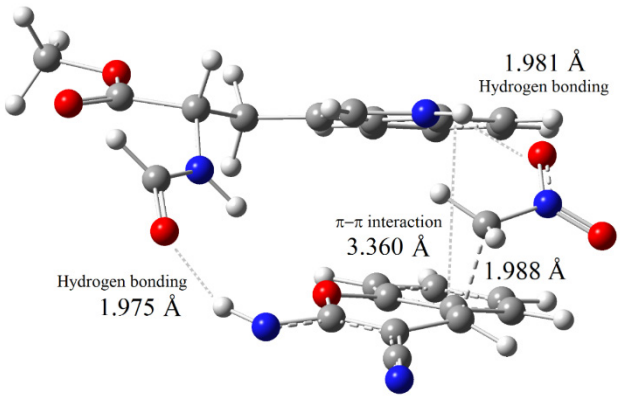

Figure 5. Optimized structure and intermolecular interactions (<3.5 Å) of the 3-TS complex molecule.

nucleophilic attack of nitromethane to 2-iminochromene substrate is the first step of the mechanism. The transition state (3-TS) formed in this step determines the rate of the reaction and plays a key role in the mechanism.

The optimized structure of the 3-TS molecule in the rate-determining step of the reaction is depicted in detail in Figure 5. The catalyst molecule coexists with the 2-iminochromene with a NH ···· O (catalyst) hydrogen bond with a length of 1.975 Å, while it forms a hydrogen bond between the nitromethane molecule and the NH ···· O (nitromethane) atoms (1.981 Å length) on the other hand. In addition, π-π interactions at a distance of 3.360 Å between the aromatic rings of the catalyst and the 2-iminochromene molecules play an important role in the stability of the transition state. The energy barrier (E_a) of this step is 63.26 $kJmol^{-1}$. The distance between C4 carbon atom of 2-iminochromene and carbon atom of nitromethane is calculated as 1.998 Å. The calculation of the single negative frequency at –548 cm^{-1} in 3-TS supports the correct optimization of the molecule. The second step of the reaction is the proton transfer step, and it takes place rapidly over 5-TS. The energy barrier in this step is calculated to be 48.99 $kJmol^{-1}$.

When the reaction mechanism is considered as a whole, the formation energy of the product 6-P is calculated as –68.93 $kJmol^{-1}$.

In conclusion, cross-linked microbeads, [poly(EGDMA-MATrp)], were successfully applied as a heterogeneous catalyst in conjugate addition reactions of nitromethane to substituted 2-iminochromenes. Experimental results revealed the activating role of hydrophobic interactions in aqueous reaction medium. We obtained the best results with 2-iminochromene substrates having electron rich aromatic rings that is able to form stronger stacking interactions with the catalyst. DFT calculations also revealed the significant role of π-π interactions as well as hydrogen bonding in the reaction mechanism. Polymeric microbeads were very durable and reused 5 times without a significant loss of activity. The design and synthesis of polymeric microbeads with more effective chiral microenvironments for asymmetric synthesis is under investigation.

Acknowledgment
We gratefully thank Bursa Technical University Scientific Research Fund (BAP 211N021) for financial support.

References

1. Sýkora D, Řezanka P, Záruba K, Král V. Recent advances in mixed-mode chromatographic stationary phases. Journal of Separation Science 2019; 42 (1): 89-129. doi: 10.1002/jssc.201801048
2. Kim S, Kim B, Dogan NA, Yavuz CT. Sustainable Porous Polymer Catalyst for Size-Selective Cross-Coupling Reactions. ACS Sustainable Chemistry & Engineering 2019; 7 (12): 10865-10872. doi: 10.1021/acssuschemeng.9b01729
3. Funke W, Okay O, Joos-Müller B. Microgels-Intramolecularly Crossünked Macromolecules with a Globular Structure. Advances in Polymer Science 1998; 136: 139-234. doi: 10.1007/3-540-69682-2_4
4. Barner L. Synthesis of Microspheres as Versatile Functional Scaffolds for Materials Science Applications. Advanced Materials 2009; 21 (24): 2547-2553. doi: 10.1002/adma.200900373
5. Steinke JHG, Dunkin IR, Sherrington DC. Transparent macroporous polymer monoliths. Macromolecules. 1996; 29 (18): 5826-5834. doi: 10.1021/ma951875e
6. Zhao W, Li A, Zhang A, Zheng Y, Liu J. Recent Advances in Functional-Polymer-Decorated Transition-Metal Nanomaterials for Bioimaging and Cancer Therapy. ChemMedChem 2018; 13 (20): 2134-2149. doi: 10.1002/cmdc.201800462
7. Yuan D, Zhang H. Nanosized palladium supported on diethylenetriamine modified superparamagnetic polymer composite microspheres: Synthesis, characterization and application as catalysts for the Suzuki reactions. Applied Catalysis A: General 2014; 475: 249-255. doi: 10.1016/J.apcata.2014.01.037
8. Ying A, Liu S, Li Z, Chen G, Yang J et al. Magnetic Nanoparticles-Supported Chiral Catalyst with an Imidazolium Ionic Moiety: An Efficient and Recyclable Catalyst for Asymmetric Michael and Aldol Reactions. Advanced Synthesis & Catalysis 2016; 358 (13): 2116-2125. doi: 10.1002/adsc.201600145
9. Ling X, Xie Y, Lin X, Li L, Qiu T. Porous polymer microsphere functionalized with benzimidazolium based ionic liquids as effective solid catalysts for esterification. The Chinese Journal of Chemical Engineering 2019; 27 (10): 2455-2466. doi: 10.1016/j.cjche.2019.01.039
10. Dadhania HN, Raval DK, Dadhania AN. Magnetically retrievable magnetite (Fe3O4) immobilized ionic liquid: An efficient catalyst for the preparation of 1-carbamatoalkyl-2-naphthols. Catalysis Science & Technology 2015; 5 (10): 4806-4812. doi: 10.1039/c5cy00849b
11. Bukowska A, Bester K, Pytel M, Bukowski W. Polymer Beads Decorated with Dendritic Systems as Supports for A3 Coupling Catalysts. Catalysis Letters 2021; 151 (2): 422-434. doi: 10.1007/s10562-020-03301-0.
12. Ullah MW, Thao NTP, Sugimoto T, Haraguchi N. Synthesis of core-corona polymer microsphere-supported cinchonidinium salt and its application to asymmetric synthesis. Molecular Catalysis 2019; 473: 110392. doi: 10.1016/j.mcat.2019.110392
13. Chen J, Ren Y, Li H, Yang W, Wu Q et al. Structural regulation of magnetic polymer microsphere@ionic liquids with an intermediate protective layer and application as core-shell-shell catalysts with high stability and activity. ACS Omega 2020; 5 (36): 23062-23069. doi: 10.1021/acsomega.0c02777
14. Osman B, Tümay Özer E, Demirbel E, Güçer Ş, Beşirli N. Synthesis and characterization of L-tryptophan containing microbeads for removal of dimethyl phthalate from aqueous phase. Separation and Purification Technology 2013; 109: 40-47. doi: 10.1016/j.seppur.2013.02.025
15. Osman B, Tümay Özer E, Kara A, Yeşilova E, Beşirli N. Properties of magnetic microbeads in removing bisphenol-A from aqueous phase. Journal of Porous Materials 2015; 22 (1): 37-46. doi: 10.1007/s10934-014-9870-z
16. Osman B, Tümay Özer E, Beşirli N, Güçer Ş. Development and application of a solid phase extraction method for the determination of phthalates in artificial saliva using new synthesised microspheres. Polymer Testing 2013; 32 (4): 810-818. doi: 10.1016/j.polymertesting.2013.03.017
17. Tümay Özer E, Osman B, Yazıcı T. Dummy molecularly imprinted microbeads as solid-phase extraction material for selective determination of phthalate esters in water. Journal of Chromatography A 2017; 1500: 53-60. doi: 10.1016/j.chroma.2017.04.013
18. Tümay Özer E, Osman B, Parlak B. An experimental design approach for the solid phase extraction of some organophosphorus pesticides from water samples with polymeric microbeads. Microchemical Journal 2020; 154: 104537. doi: 10.1016/j.microc.2019.104537
19. Tümay Özer E, Osman B, Kara A, Demirbel E, Beşirli N et al. Diethyl phthalate removal from aqueous phase using poly(EGDMA-MATrp) beads: Kinetic, isothermal and thermodynamic studies. Environmental Technology 2015; 36 (13): 1698-1706. doi: 10.1080/09593330.2015.1006687
20. DiLabio GA., Johnson ER. Lone Pair–π and π–π Interactions Play an Important Role in Proton-Coupled Electron Transfer Reactions. Journal of the American Chemical Society 2007; 129 (19): 6199-6203. doi: 10.1021/ja068090g
21. Peris E. Polyaromatic N-heterocyclic carbene ligands and pi-stacking. Catalytic consequences. Chemical Communications 2016; 52: 5777. doi: 10.1039/c6cc02017h

22. Ruiz-Botella S, Peris E. Unveiling the Importance of π-Stacking in Borrowing-Hydrogen Processes Catalysed by Iridium Complexes with Pyrene Tags. Chemistry-A European Journal 2015; 21 (43): 15263-15271. doi: 10.1002/chem.201502948

23. Mazzonna M, Bietti M, Dilabio GA, Lanzalunga O, Salamone M. Importance of π-stacking interactions in the hydrogen atom transfer reactions from activated phenols to short-lived N-oxyl radicals. The Journal of Organic Chemistry 2014; 79 (11): 5209-5218. doi: 10.1021/jo500789v

24. Wang Y, Zhang SR, Wang Y, Qu LB, Wei D. Insights into the NHC-catalyzed cascade Michael/aldol/lactamization reaction: Mechanism and origin of stereoselectivity. Organic Chemistry Frontiers 2018; 5 (13): 2065-2072. doi: 10.1039/c8qo00398j

25. China Raju B, Nageswara Rao R, Suman P, Yogeeswarib P, Sriramet D et al. Synthesis, structure–activity relationship of novel substituted 4H-chromen-1,2,3,4-tetrahydropyrimidine-5-carboxylates as potential anti-mycobacterial and anticancer agents. Bioorganic & Medicinal Chemistry Letters 2011; 21 (10): 2855-2859. doi: 10.1016/j.bmcl.2011.03.079

26. Sabry NM, Mohamed HM, Khattab ESAEH, Motlaq SS, El-Agrody AM. Synthesis of 4H-chromene, coumarin, 12H-chromeno[2,3-d] pyrimidine derivatives and some of their antimicrobial and cytotoxicity activities. European Journal of Medicinal Chemistry 2011; 46 (2): 765-772. doi: 10.1016/j.ejmech.2010.12.015

27. Singh OM, Devi NS, Thokchom DS, Sharma GJ. Novel 3-alkanoyl/aroyl/heteroaroyl-2H-chromene-2-thiones: Synthesis and evaluation of their antioxidant activities. European Journal of Medicinal Chemistry 2010; 45 (6): 2250-2257. doi: 10.1016/j.ejmech.2010.01.070

28. Bhavsar D, Trivedi J, Parekh S et al. Synthesis and in vitro anti-HIV activity of N-1,3-benzo[d]thiazol-2-yl-2- (2-oxo-2H-chromen-4-yl)acetamide derivatives using MTT method. Bioorganic & Medicinal Chemistry Letters 2011; 21 (11): 3443-3446. doi: 10.1016/j.bmcl.2011.03.105

29. Li W, Liu H, Jiang X, Wang J. Enantioselective organocatalytic conjugate addition of nitroalkanes to electrophilic 2-iminochromenes. ACS Catalysis 2012; 2 (8): 1535-1538. doi: 10.1021/cs300313j

30. Patel JP, Avalani JR, Raval DK. Polymer supported sulphanilic acid: A highly efficient and recyclable green heterogeneous catalyst for the construction of 4,5-dihydropyrano[3,2-c] chromenes under solvent-free conditions. Journal of Chemical Sciences 2013; 125 (3): 531-536. doi: 10.1007/s12039-013-0408-8

31. Gupta V, Singh RP. Enantioselective vinylogous Michael addition of β,γ-unsaturated butenolide to 2-iminochromenes. New Journal of Chemistry 2019; 43 (25): 9771-9775. doi: 10.1039/c9nj01584a

32. Pourjavadi A, Hosseini SH, Emami ZS. Cross-linked basic nanogel; robust heterogeneous organocalayst. Chemical Engineering Journal 2013; 232: 453-457. doi: 10.1016/j.cej.2013.07.090

33. Kalla RMN, Varyambath A, Kim MR, Kim I. Amine-functionalized hyper-crosslinked polyphenanthrene as a metal-free catalyst for the synthesis of 2-amino-tetrahydro-4H-chromene and pyran derivatives. Applied Catalysis A: General 2017; 538: 9-18. doi: 10.1016/j.apcata.2017.03.009

34. Mohammadi P, Sheibani H. Synthesis and characterization of Fe3O4@SiO2 guanidine-poly acrylic acid nanocatalyst and using it for one-pot synthesis of 4H-benzo[b]pyrans and dihydropyrano[c]chromenes in water. Materials Chemistry and Physics 2019; 228: 140-146. doi: 10.1016/j.matchemphys.2018.11.058

35. Siddiqui S, Siddiqui ZN. Copper Schiff base functionalized polyaniline (Cu-SB/PANI): A highly efficient polymer based organometallic catalyst for the synthesis of 2-amino chromene derivatives. Applied Organometallic Chemistry 2019; 33 (10). doi: 10.1002/aoc.5161

36. Jadhav SN, Patil SP, Sahoo DP, Rath D, Parida K et al. Organocatalytic Cascade Knoevenagel–Michael Addition Reactions: Direct Synthesis of Polysubstituted 2-Amino-4H-Chromene Derivatives. Catalysis Letters 2020; 150 (8): 2331-2351. doi: 10.1007/s10562-019-03089-8

37. Koz G, Koz O, Coskun N. Enantioselective synthesis of 2-amino-4-(nitromethyl)-4H-chromene-3-carbonitriles from 2-iminochromenes. Synthetic Communications 2016; 46 (10): 909-915. doi: 10.1080/00397911.2016.1177728

38. Koz G, Koz Ö. DBU-catalyzed synthesis of novel 2-Amino-3-nitrile-4H-chromenes. Zeitschrift fur Naturforschung - Section B Journal of Chemical Sciences 2017; 72 (9): 647-653. doi: 10.1515/znb-2017-0040

39. Li W, Huang J, Wang J. Organocatalytic conjugate addition promoted by multi-hydrogen-bond cooperation: Access to chiral 2-amino-3-nitrile-chromenes. Organic and Biomolecular Chemistry 2013; 11 (3): 400-406. doi: 10.1039/c2ob27102h

40. Volmajer J, Toplak R, Leban I, Le Marechal AM. Synthesis of new iminocoumarins and their transformations into N-chloro and hydrazono compounds. Tetrahedron 2005; 61 (29): 7012-7021. doi: 10.1016/j.tet.2005.05.020

41. Dong W, Xu D, Xie J. Aqueous-mediated michael addition of active methylene compounds with nitroalkenes. Chinese Journal of Chemistry 2012; 30 (8): 1771-1774. doi: 10.1002/cjoc.201200228

42. Lv W, Guo C, Dong Z, Tang S, Liu B, Dong C. C3-Symmetric cinchonine-squaramide as a recyclable efficient organocatalyst for tandem Michael addition–cyclisation of malononitrile and nitrovinylphenols. Tetrahedron Asymmetry 2016; 27 (14-15): 670-674. doi: 10.1016/j.tetasy.2016.05.011

43. Hu K, Lu A, Wang Y, Zhou Z, Tang C. Chiral bifunctional squaramide catalyzed asymmetric tandem Michael-cyclization reaction: Efficient synthesis of optically active 2-amino-4H-chromene-3-carbonitrile derivatives. Tetrahedron Asymmetry 2013; 24 (15-16): 953-957. doi: 10.1016/j.tetasy.2013.07.010

44. Grimme S, Antony J, Ehrlich S, Krieg H. A consistent and accurate ab initio parametrization of density functional dispersion correction (DFT-D) for the 94 elements H-Pu. The Journal of Chemical Physics 2010; 132 (15). doi: 10.1063/1.3382344